AIP | Conference Proceedings

Thermal modelling comparing high temperature fixed point measurements by contact and non-contact thermometry

P. Castro, G. Machin, and J. V. Pearce

Citation: AIP Conf. Proc. **1552**, 358 (2013); doi: 10.1063/1.4821387
View online: http://dx.doi.org/10.1063/1.4821387
View Table of Contents: http://proceedings.aip.org/dbt/dbt.jsp?KEY=APCPCS&Volume=1552&Issue=1
Published by the AIP Publishing LLC.

Thermal Modelling Comparing High Temperature Fixed Point Measurements by Contact and Non-Contact Thermometry

P. Castro[1], G. Machin[2], and J. V. Pearce[2]

[1]University of Cantabria, Avenida de los Castros s/n, 39005, Santander, Cantabria, Spain
[2] National Physical Laboratory, Hampton Rd., Teddington, Middlesex, TW11 0LW, UK

Abstract. This paper reports thermal modelling that aims to establish if the measurement method - either by a radiation thermometer or by a thermocouple - significantly influences the measured temperature of the high temperature fixed points Co-C, Pd-C and Ru-C. It is clear that both measurement techniques have specific physical characteristics which may affect the temperature measured during the melting plateau. With the radiation thermometer, the radiation heat transfer is directly influenced by the environment because the back-wall is effectively viewing the cold outside environment. In the case of a thermocouple direct viewing of the outside world is blocked so radiation transport is significantly reduced; however, in the case of the thermocouple there is a different component of heat transfer, namely conduction from the thermowell walls in contact with the thermocouple along the thermocouple stem itself.

Keywords: Thermal modelling, radiation thermometer, thermocouple, melting plateau, high temperature fixed points, HTFP

INTRODUCTION

This paper reports thermal modelling that aims to establish if the measurement method, either by a radiation thermometer or by a thermocouple, significantly influences the measured temperature of high temperature fixed points (HTFPs). The modelling is performed at the melting temperatures of Co-C, Pd-C and Ru-C HTFPs. To begin with, a simple model calculation using an NPL cell design was performed. Then, the influence of the furnace environment was taken into account with the experimental temperature profile measured by the thermocouple along the central well being introduced as an input into the thermal model.

It is clear that both measurement techniques have specific physical characteristics which may affect the temperature measured during the melting plateau. With the radiation thermometer, the radiation heat transfer is directly influenced by the environment because the back-wall is effectively viewing the outside environment. In the case of a thermocouple direct viewing of the outside world is blocked and so radiation transport is eliminated by the presence of the thermocouple. However in this case heat transfer by conduction is important. This arises because the thermowell walls are in thermal contact with the thermocouple, either directly or via the surrounding gas.

These differences in heat transport are the main reasons why it is possible that the thermocouple may yield a different temperature for a HTFP to that measured with a radiation thermometer. The question to be answered is: does the heat loss by radiance (temperature drop) exceed the heat loss by conduction (along the thermocouple)? If so the radiation thermometer would measure lower temperatures than the thermocouple method. This effect may become more significant as the nominal temperature of the HTFP increases as radiation losses increase with the fourth power of temperature but conduction has a linear behaviour.

1. DESCRIPTION OF THE MODELS

Two different HTFP designs in two different furnaces were studied. The first cell (figure 1) is used in thermocouple calibrations [1], and overall it is 120.8 mm long, other dimensions are given on the figure.

Temperature: Its Measurement and Control in Science and Industry, Volume 8
AIP Conf. Proc. 1552, 358-362 (2013); doi: 10.1063/1.4821387
2013 AIP Publishing LLC 978-0-7354-1178-4/$30.00

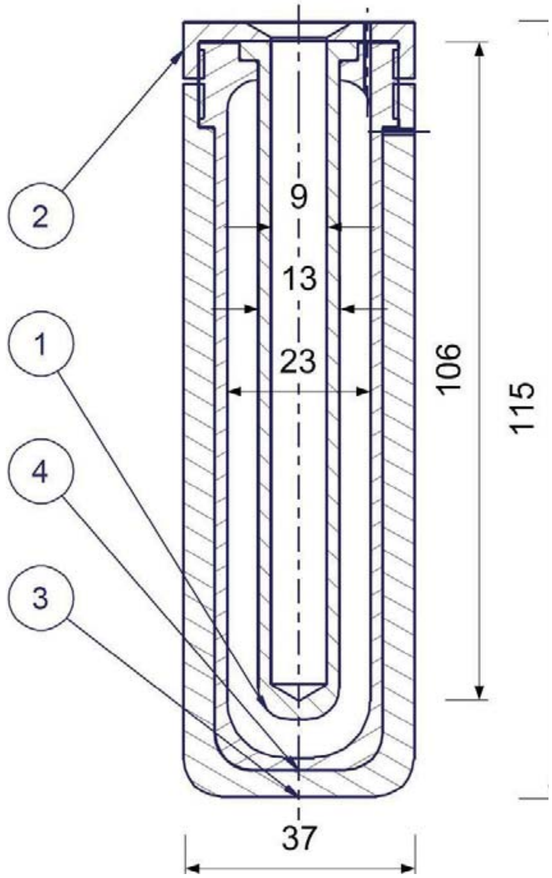

FIGURE 1. NPL HTFP cell design for thermocouple calibration. 1: thermowell, 2: top cap, 3: outer sleeve, 4: inner sleeve. Units in mm.

The first thermal model of this cell was constructed without any furnace, i.e. its aperture is looking directly to the outside environment, with a uniform temperature profile applied to the outside wall. The second thermal model included the effect of the furnace used to realize the HTFP cell for thermocouple calibrations. For this second configuration the HTFP cell was inside a second graphite cylinder 147 mm long and 63 mm external diameter, which acted as a heat thermalisation block. This in turn was placed in an alumina tube with 400 mm of graphite felt discs above the cell and a uniform aperture diameter of 9 mm beyond the cell to allow for insertion of the thermocouple. A schematic diagram of the fixed point assembly is shown in figure 2. The fixed point is realized in a three zone furnace with a temperature gradient of less than 1 K over the length of the cell with the top of the cell slightly hotter than the bottom.

Two fixed points were evaluated in this cell-furnace configuration: the Co-C point (1597 K) and the Pd-C point (1765 K). The furnace temperature profile for the Co-C point was obtained from experimental measurements. In this case the furnace was stepped 16 K above the melting point and the temperature profile measured at a temperature just below the HTFP melting temperature. This profile was then used as an input to the thermal model, being that of the internal well of the furnace. For the thermal model of the Pd-C the same furnace profile shape as that of the Co-C point was used, again starting with a step of 16 K above the melting point.

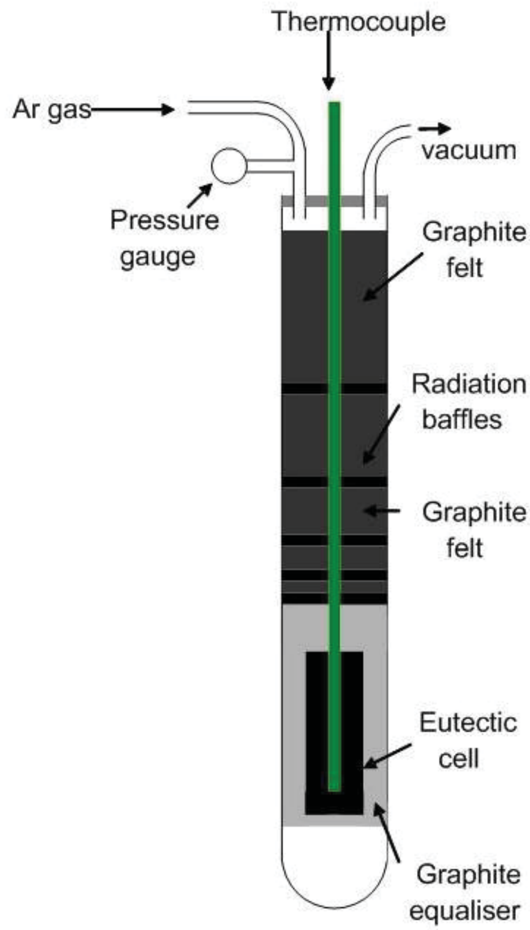

FIGURE 2. Schematic diagram of the cell holder and its assembly used for thermocouple calibrations.

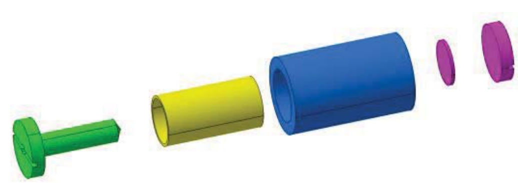

FIGURE 3. NPL HTFP design. Total length 40 mm. Internal cavity length 28.5 mm. Internal diameter 3 mm.

The second cell is the NPL design [2], called mark V, of 40 mm length and 3 mm internal diameter (figure 3). This design of cell is primarily for radiation thermometry measurements. The cell was first simulated without any furnace and then inside a Thermogauge furnace with 35 mm of graphite foams and discs in front and behind the blackbody. In addition the insulation at the front with a clear aperture tapered from 3 mm at the blackbody aperture to 12 mm at the end of the insulation. With this configuration the Ru-C point (2226 K) was studied.
In this case the furnace temperature profile was assumed as constant, at 16 K above the nominal melting temperature of Ru-C. More details of the model can be found in [2].

2. THERMAL MODELLING

The crucibles and furnaces were modelled with a 2D design made by ANSYS FLUENT, a computational fluid dynamics software based on finite volumes and used in previous studies in this field [3, 4]. The model describes the heat transport by conduction and radiation in a transient state during the melting of the fixed point.

The main initial and boundary conditions were:
- The initial starting point for the model was 20 K below the melting point.
- The boundary condition in the external wall of the crucible in the cases without a furnace was fixed at 16 K above the melting temperature.
- The temperature profiles for the first (thermocouple) furnace were introduced from the measured experimental temperatures (figure 4).
- For the Thermogauge furnace, a constant temperature profile of 16 K above the Ru-C melting point was fixed in the external wall of the furnace. It is recognized that this is an optimistic assumption. However previous modelling [2, 5] showed that only a few mK (Co-C) and few x 10 mK (Ru-C) difference was observed between using a flat profile as here and a more extreme profile which approached ambient at the front of the furnace; hence this simplifying assumption is justified.

The thermal properties of several materials were required to facilitate the model in this study: those of the fixed point metals (Co, Pd and Ru), graphite, graphite foams, Pt, alumina and argon. The thermal properties used for these materials are given in table 1. The thermal conductivity value for graphite is taken from [6]. The emissivity of solid graphite and graphite foams is from [7]. The heat capacity, thermal conductivity, latent heat and density values of the fixed point metals are those from the pure metals at room temperature.

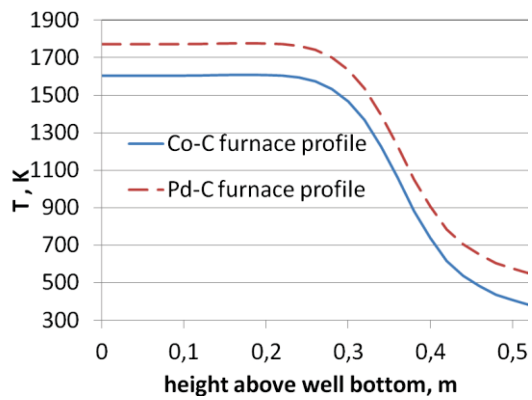

FIGURE 4. Furnace temperature profile for Co-C and Pd-C points.

TABLE 1. Material Properties.

	Cp, J kg^{-1} K^{-1}	*k*, W m^{-1} K^{-1}	*ρ*, kg m^{-3}	emissivity	Latent heat, kJ.kg^{-1}	Viscosity, kg.m^{-1}.s^{-1}	melting *T*, K
Co-C	456	45	7200		274407	100	1596.4
Pd-C	244	72	12023		157301	100	1764.8
Ru-C	238.05	117	12450		381814.6	100	2226
Pt	170	92	21090				
Graphite	690	53.6	2250	0.86			
Foams	370	0.35	50	0.86			
Alumina	1300	6.08	3900	0.4			
Argon	520.64	0.0158	1.6228				

3. RESULTS

3.1. Thermocouple Cell and Vertical Furnace

Two different fixed points (Co-C and Pd-C) were studied in this configuration. The melting plateaux for the bare cell and the cell inside the furnace are shown in figures 5, 6, 7 and 8, determined for measurements using both a thermocouple and a radiation thermometer.

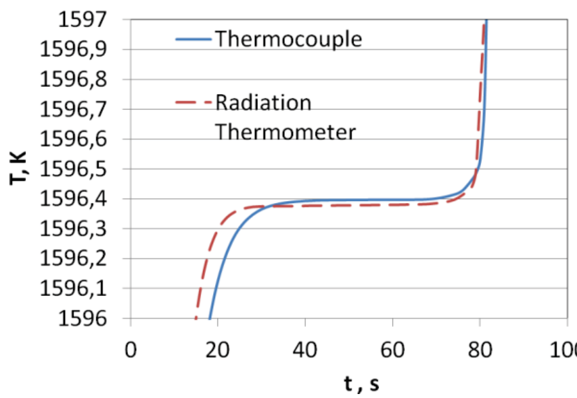

FIGURE 5. Melting plateau for Co-C in the cell without furnace.

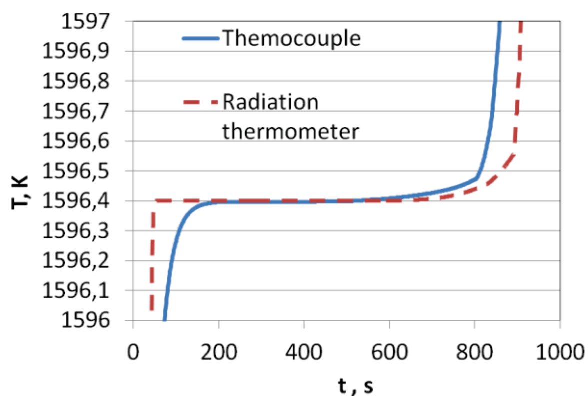

FIGURE 6. Melting plateau for Co-C in the cell inside the furnace.

It can be seen that for the bare crucible there were differences between the temperature measured by the thermocouple and the one measured by the radiation thermometer. In the latter case the melting started earlier and the flat part of the plateau was about 20 mK lower than in the thermocouple case. For the Pd-C this difference increased to 26 mK.

However when the influence of the furnace was taken into account, it is observed that the melting plateau measured with the radiation thermometer continued to start earlier but the differences in the point of inflexion of the plateau have effectively disappeared, within the limits of resolution of the model.

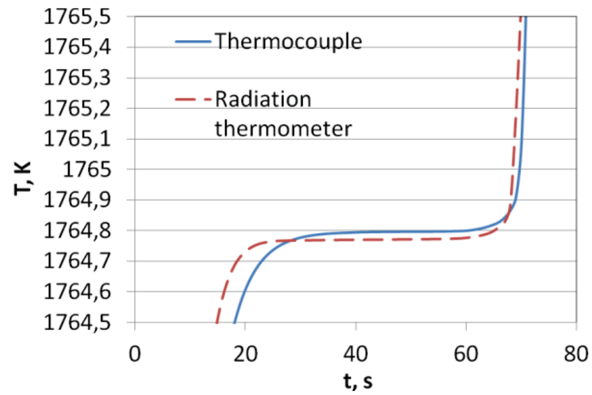

FIGURE 7. Melting plateau for Pd-C in the cell without furnace.

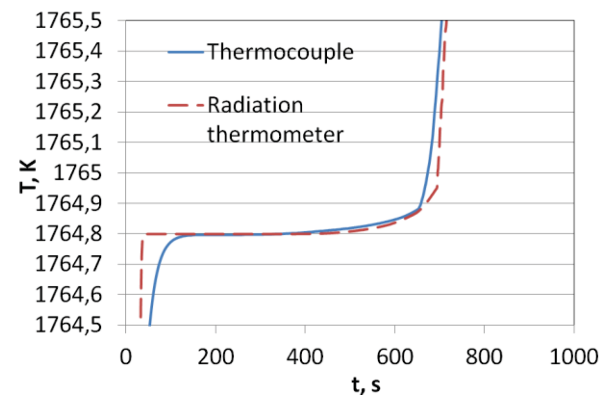

FIGURE 8. Melting plateau for Pd-C in the cell inside the furnace.

3.2. Mark V Cell and Thermogauge Furnace

This configuration was studied for the Ru-C point in two different cases, the bare crucible and the crucible inside a uniform Thermogauge furnace.

The melting plateaux for the bare cell and the cell inside the furnace are shown in figures 9 and 10.

In this case, for both the bare crucible and the crucible inside the furnace, a lower melting temperature was measured for the case of radiation thermometer. However the temperature difference was about 80 mK for the bare cell and about 30 mK for the cell inside the furnace. This is thought to be due to the fact that in this case the HTFP crucible is much closer to the ambient environment than in the case of the contact thermometry cell.

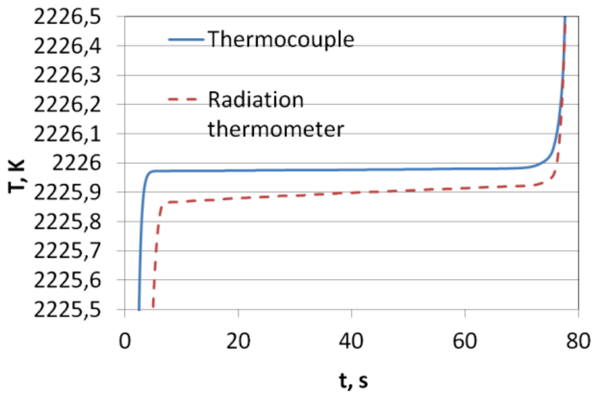

FIGURE 9. Melting plateau for Ru-C in the cell without furnace.

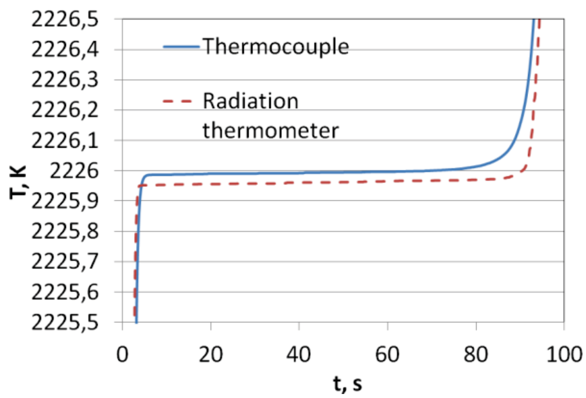

FIGURE 10. Melting plateau for Ru-C in the cell inside the furnace.

4. CONCLUSIONS

The main conclusions of this paper are:

- In the extreme case, which is the bare crucible without any furnace environment, radiation losses are shown to be slightly higher than conduction losses, with the difference between the two being equivalent to a different in melting temperature of 20 mK for Co-C, 26 mK for Pd-C and 80 mK for Ru-C.

- If the effect of the furnace is taken into account, for the case of the vertical furnace with a real temperature profile along it, there is no resolvable difference between the temperature measured by a thermocouple and that measured by a radiation thermometer.

- In the case of the Thermogauge furnace with the higher temperature fixed point of Ru-C there is a very small difference (about 30 mK) between the thermocouple and radiance temperature measurements. The value of the difference is insignificant compared to any other uncertainties likely to be experienced when using these fixed points for calibrating thermocouples.

- This work suggests that, provided the temperatures of HTFPs are determined from cells incorporating good (ie high emissivity) blackbody cavities, their assigned temperatures could be used directly for contact thermometry purposes.

- It is clear that the furnace environment effectively (or largely) eliminates the differences between both thermometry methods even for fixed points up to 2200 K.

REFERENCES

1. Pearce, J. V., Lowe, D. H., Head, D. I. and Machin, G. "Optimizing Contact Thermometry High-Temperature Fixed-Point Cells (>1.100 ºC) Using Finite-Element Analysis". *Int. J. Thermophys.* **29**, pp. 250-260 (2008).
2. Castro, P., Machin, G., Villamañan, M. A. and Lowe, D. "Calculation of the Temperature Drop for High-Temperature Fixed Points for Different Furnace Conditions". *Int. J. Thermophys.* **32**, pp. 1773-1785 (2011).
3. Machin, G., Castro, P., Levick, A. and Villamañan, M. A. "Temperature Effects of Imperfectly Formed Metal-Ingots in High Temperature Fixed Point Crucibles". *Measurement* **44**, pp. 738-742 (2011).
4. Bloembergen, P., Hanssen, L. M., Mekhontsev, S. N., Castro, P. and Yamada, Y. "A Determination Study of the Cavity Emissivity of the Eutectic Fixed Points Co-C, Pt-C and Re-C". *Int. J. Thermophys.* **32**, pp. 2623-2632 (2011).
5. Castro, P., Bloembergen, P., Yamada, Y., Villamañan, M. A. and Machin, G. "On the Uncertainty in the Temperature Drop across the Backwall of High-Temperature Fixed Points". *Acta Metrologica Sinica* **29**, pp. 253-260 (2008).
6. Touloukian, Y. S., Powell, R. W., Ho, C. Y. and Klemens, P. G., "Thermal Conductivity: Nonmetallic Solids". *Thermophysical Properties of Matter, TPRC Data Series*, **2** (IFI/Plenum, New York), pp. 585–588 (1970).
7. Fischer, J. and Jung, H. J. "Determination of the Thermodynamic Temperatures of the Freezing Points of Silver and Gold by Near Infrared". *Metrologia* **26**, pp. 245 (1989).